Effect of α- and β-Nucleating Agents on the Fracture Behavior of Polypropylene-*co*-ethylene

Shi-Wei Wang,[1] Wei Yang,[1,2] Guan Gong,[1] Bang-Hu Xie,[1] Zheng-Ying Liu,[1] Ming-Bo Yang[1]

[1]*College of Polymer Science and Engineering, Sichuan University, State Key Laboratory of Polymer Materials Engineering, Chengdu 610065, Sichuan, People's Republic of China*
[2]*The Key Laboratory of Polymer Processing Engineering, Ministry of Education, South China University Technology, Guang Zhou 510640, People's Republic of China*

Received 11 May 2007; accepted 4 September 2007
DOI 10.1002/app.27678
Published online 7 January 2008 in Wiley InterScience (www.interscience.wiley.com).

ABSTRACT: The effect of α- and β-nucleating agents (NA) of various amounts on the fracture behavior of polypropylene-*co*-ethylene (CPP) was evaluated using the essential work of fracture (EWF) method. The specific EWF values of CPPs incorporated with α-NA of different amount were all lower than that of pure CPP, while the specific nonessential work of fracture was the highest at relative low α-NA loading (0.1 wt %), and then decreased with further increasing amount of α-NA. Similar trend of variation was observed with increasing amount of β-NA in CPP, and it was found that the variation of K_β for β-NA nucleated CPP versus NA content accorded well with the EWF versus NA content, which indicated that the addition of β-NA could lead to effectively increased β-crystal content and consequently improved fracture resistance of CPP. © 2008 Wiley Periodicals, Inc. J Appl Polym Sci 108: 591–597, 2008

Key words: polypropylene-*co*-ethylene; nucleating agent; crystal structure; fracture behavior

INTRODUCTION

Polypropylene-*co*-ethylene (CPP) is a versatile semicrystalline polymer used in a wide variety of applications. The interrelation between structures, especially the crystalline structures, and mechanical behavior of CPP as well as its blends or composites, has been reported in many literatures.[1–9] The crystallization process of polymer includes two stages, that is, nucleation and crystal growth. Nucleation involves the orientation of the loose coiled polymer chains into proper conformation, while in the process of crystal growth, polymer chains grow on the nuclei in a three-dimensional pattern and in most case, form a spherical crystal cluster which is called a spherulite. Nucleation in polymers may be homogeneous or heterogeneous. Homogeneous nucleation occurs at high degree of super-cooling, while heterogeneous nucleation occurs at relatively low degree of super-cooling and often with the addition of a foreign body called nucleating agents (NAs) which reduces the free energy barrier for nucleation.[10] It is well-known that NA can increase the number of crystallization sites and reduce the spherulite size. Many articles have reported the enhanced physical properties of semicrystalline polymers such as impact strength and surface gloss when the crystallites' size become smaller as a result of NA addition.

The essential work of fracture (EWF) method has gained great interest in recent years for its special applicability in studying the fracture performance of ductile polymer products, especially for sheets and films.[11–19] The EWF concept was first proposed by Broberg[20] and then developed by Cotterell and coworkers,[21–23] Mai and coworkers,[22–27] Cotterell and Reddel,[21] and Karger-Kocsis[28–35] et al. According to the EWF theory,[22–35] the total energy required to fracture a precracked specimen can be partitioned into the EWF, w_e and the nonessential work of fracture, w_p. w_e is a surface energy dissipated in the inner fracture process zone (IFPZ), and w_p is a volume energy dissipated in the outer plastic deformation zone (OPDZ). The deep double edge-notched tension (DDENT) sample used for EWF tests to show the different energy dissipation zones is presented in Figure 1. For a given thickness, w_e is proportional to the ligament length, l, and w_p is propor-

Correspondence to: M. B. Yang (yangmb@scu.edu.cn) or W. Yang (ysjsanjin@163.com).

Contract grant sponsor: National Natural Science Foundation of China; contract grant numbers: 20734005, 50503014, and 50533050.

Contract grant sponsor: National Ministry of Education, China (Doctoral Research Foundation); contract grant number: 20060610029.

Contract grant sponsor: Special Funds for Major Basic Research; contract grant number: 2005CB623808.

Contract grant sponsor: Opening Project of The Key Laboratory of Polymer Processing Engineering, Ministry of Education, China.

© 2008 Wiley Periodicals, Inc.
WILEY InterScience® DISCOVER SOMETHING GREAT

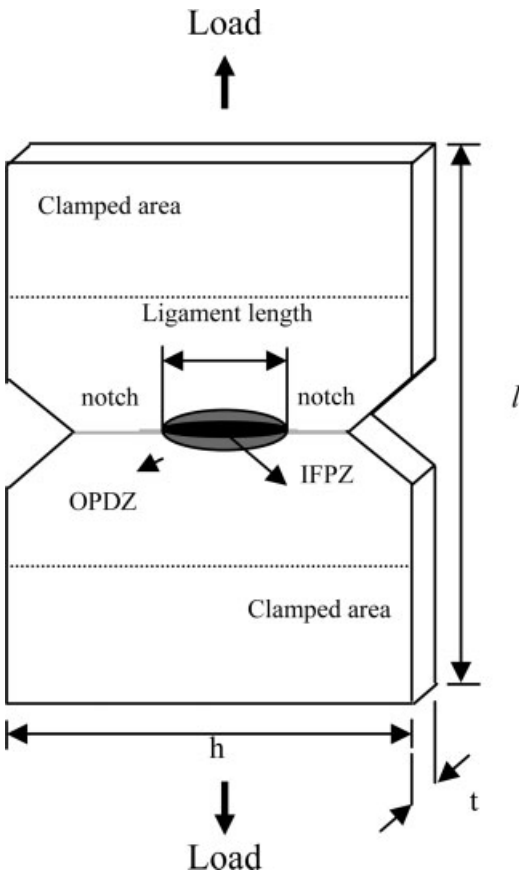

Figure 1 DDENT sample used for EWF test.

tional to l^2. Thus the fracture energy can be written as follows:

$$w_f = w_e\, lt + \beta w_p l^2 t \tag{1}$$

$$w_f = w_f/lt = w_e + \beta w_p l \tag{2}$$

where w_f is the special total work of fracture, w_e and w_p being the specific EWF and specific nonessential work of fracture, respectively, l the ligament length, t the specimen thickness, and β the shape factor associated with the plastic zone. According to eq. (2), w_e and βw_p can be obtained from the intercept and slope of the regression line to zero ligament, respectively.

To find out the energy distribution during the fracture process, a method of partition between the specific work of fracture for yielding and for necking and subsequent fracture[36] is also employed in the present article, making the peak of the load-displacement curves as the cut-off point, as shown in Figure 2. As the composed terms were under plane stress conditions, eq. (1) can be rewritten as follows:

$$w_f = w_y + w_n \tag{3}$$

$$w_y = w_{e,y} + \beta' w_{p,y} l \tag{4}$$

$$w_n = w_{e,n} + \beta'' w_{p,n} l \tag{5}$$

where $w_{e,y}$ and $w_{e,n}$, are the yielding and the necking and subsequent fracture-related parts of the specific EWF, respectively; $\beta' w_{py}$ and $\beta'' w_{pn}$ are the yielding and the necking and subsequent fracture components of the nonspecific EWF, respectively.

Till now, EWF method has been successfully used to characterize the fracture properties of polyolefin as well as their blends and composites.[2,4,6,8,9,12,13] In this article, we focus on the effect of α- and β-NAs and their concentration on the fracture properties of CPP. The EWF parameters in the stage of yielding and sequent stage of necking and tearing are also measured to analyze the distribution of fracture energy of nucleated PP.

EXPERIMENTAL

Material

The CPP (K8303) was a granular material of propylene-*block*-ethylene copolymer produced by Beijing Yanshan Petrochemical (People's Republic of China), with 17.8 mol % of ethylene and a melt-flow rate of 1.39 g/10 min (measured at 230°C and 2.16 kg). Two kinds of NAs were used. The α-NA Millad 3988, a kind of dibenzylidene sorbitol derivatives, was produced by Milliken Chemical Europe NV. The β-NA WBG-II, a kind of rare earth organic complexes, was produced by Guangdong Winner Functional Materials (People's Republic of China).

Sample preparation

To compare the effect of α- and β-NAs on the fracture performance of nucleated CPP, the weight percentage of both NAs was set as 0, 0.1, 0.3, and 0.5 wt %. The CPP resin and NAs at preselected mass ratio were melt-blended in a SHJ-20 corotating twin-screw extruder made by Nanjing Giant Electromechanical (People's Republic of China). The barrel temperature was set in the range of 180–230°C. The extrudate

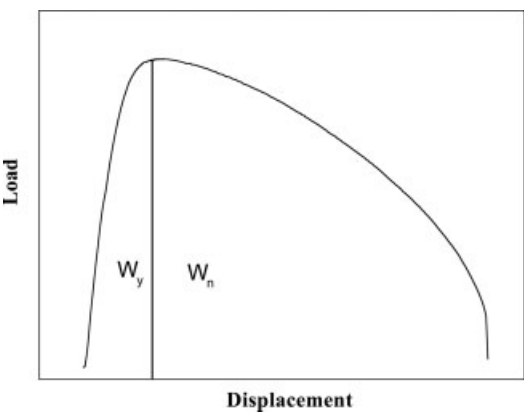

Figure 2 Energy partition of DDENT specimen.

was pelletized after extrusion and, after drying to remove the attached moisture during extrusion and pelletizing, the pellets were injected into both dumbbell and rectangular-shaped samples of 4-mm thickness on a PS40E5ASE (Nissei) precise injection molding machine. The temperature profile was 180, 210, 230, 225°C from the feeding zone to the nozzle, and both the injection and holding pressures were 50.0 MPa. Then the rectangle samples were compression-molded into sheets of about 0.5-mm thickness at 200°C and 10 MPa. The DDENT specimens (length × width = 100 mm × 35 mm), shown in Figure 1, were cut from the compression-molded sheets. The sharp precracks on both sides of the specimens were made perpendicularly to the tensile direction with a fresh razor blade. The ligament lengths and the thickness were measured before the test using a microscope and a vernier caliper, respectively.

Tests

DSC

The DSC scanning of the samples were carried out using a 204 DSC, NETZSCH instruments, in a nitrogen atmosphere, in the temperatures range of 80–200°C. The calibration of the temperature and heat flow scales at the same heating rate was performed with indium. To determine the melting behaviors of CPP with and without NA, the scanning speed was set as 10°C/min from 80 to 200°C.

WAXD

The WAXD tests of the samples were carried out on a Philips X'Pert pro MPD instrument. A conventional Cu Kα X-ray tube at a voltage of 40 kV and a filament current of 40 mA was used to obtain WAXD spectra. The scanning 2θ range is from 0 to 45° with a scanning rate of 5°/min.

EWF test

Tension of the DDENT specimens was performed on an Instron electrical universal testing machine series IX at 25°C, with a crosshead speed of 5 mm/min. The load-displacement curves were recorded and the absorbed energy until failure was calculated by computer integration of the loading curves.

RESULTS AND DISCUSSION

Load-displacement curve

The load-displacement curves during DDENT tests as a function of ligament length are shown in Figure 3. For CPP incorporated with both NAs of different content, the load-displacement curves were self-similar in shape, regardless of the ligament length. The load increases quickly with a slight increase of the displacement before the definite upper point in the initial stage. After the peak, a smooth and slow drop in the load occurred with further increase of the displacement and then the rapid load drop at the end stage of the curves signaling the fracture of the specimens. However, for both types of NAs especially for the β-NA nucleated CPPs, the load drop after yielding became faster with increasing amount of NA content.

Fracture parameters

The w_f-l diagrams gave good linear relationship for both types and various content of NAs-incorporated CPP samples, as proved by the high-linear regression coefficient in Table I. The values of w_e and βw_p, and the results for splitting the essential and nonessential work of fracture as yielding and necking terms were also listed in Table I, which were obtained by plotting w_y and w_n versus l, respectively. From Table I, it was quite clear that the w_e values of CPP incorporated with α-NA with different amount were all lower than that of pure CPP, indicating the impaired crack resistance. The w_e value of 0.1 wt % α-NA nucleated CPP was nearly only a half of that of pure CPP. However, an increase instead of gradual reduction of the w_e values was observed with further increase of α-NA amount. When the content of α-NA reached 0.5 wt %, the w_e values of the nucleated CPP was just 3 kJ/m^2 lower than that of neat CPP. This fact was due to the increase of the crystallinity induced by increase of the NA content.[14] With the increase of crystallinity, the crystal lattices were arranged more closely, so the crack resistance was improved. This fact was also validated by the crystallinity data obtained from the DSC test listed in Table II. However, the βw_p behaved contrary to w_e with increasing amount of α-NA. It was shown that the βw_p was the highest at relative low α-NA loading (0.1 wt %), while decreased with further increasing amount of NA, and nearly 2 MJ/m^3 lower than that of neat CPP at 0.5 wt % of α-NA.

Similar trend of variation for both w_e and βw_p with increasing amount of β-NAs was observed. But there were some difference worth to be noted between the fracture properties of modified CPP with both NAs, though at the same content. As can be seen, the fracture toughness of 0.1 wt % β-NA modified CPP was only 4 kJ/m^2 lower than that of pure CPP, which was nearly 10 kJ/m^2 higher than that of modified CPP with same content of α-NA. Then the w_e values increased remarkably with β-NA content, which was much higher than that of pure CPP at 0.3 wt % β-NA and finally, 10 kJ/m^2 higher

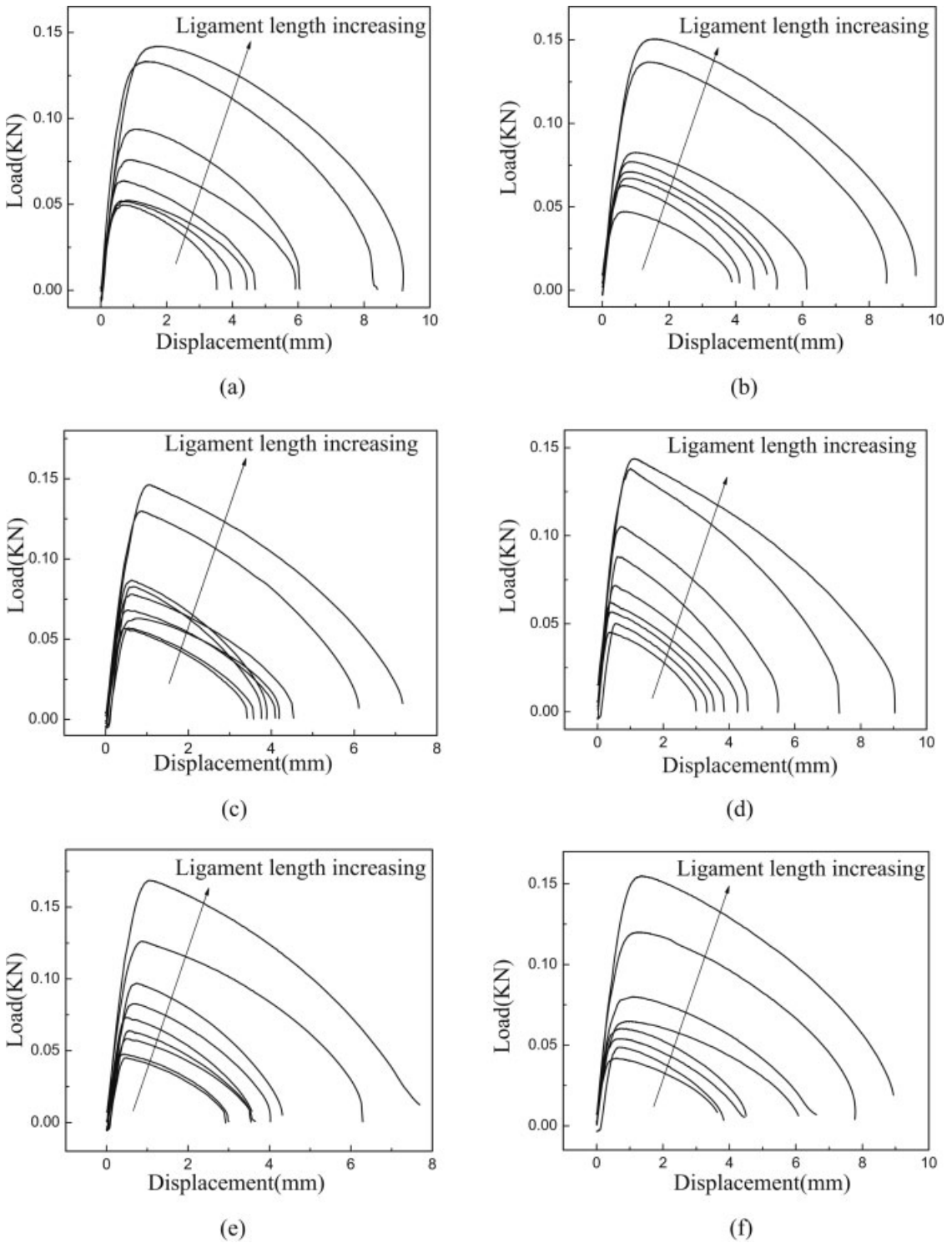

Figure 3 A plot of the load versus displacement of CPP incorporated with (a) 0.1% α-NA, (b) 0.1% β-NA, (c) 0.3% α-NA, (d) 0.3% β-NA, (e) 0.5% α-NA, and (f) 0.5% β-NA.

than that of neat CPP at 0.5 wt % β-NA. Similarly, the fluctuation of the plastic work for β-nucleated CPP was also fiercer than that of α-NA nucleated CPP. However, at the highest amount of β-NA used in this article, the βw_p value of modified CPP was appreciably higher instead of lower than that of pure CPP for α-NA nucleated CPP.

As shown in Table I, the variation of w_{en} and $\beta'' w_{pn}$ with increasing NA content for both α- and β-NAs nucleated CPP was absolutely the same as that

TABLE I
Fracture Parameters Obtained from EWF Test for Nucleated CPP with α- and β-NA of Different Content

NA content (wt %)	w_f			w_y			w_n		
	w_e (kJ/m^2)	βw_p (MJ/m^3)	R	w_{ey} (kJ/m^2)	$\beta' w_{py}$ (MJ/m^3)	R	w_{en} (kJ/m^2)	$\beta'' w_{pn}$ (MJ/m^3)	R
0	29.84	8.20	0.930	0.59	1.51	0.977	27.68	6.86	0.965
0.1α	16.29	9.46	0.933	1.05	1.27	0.986	15.23	8.19	0.984
0.3α	20.57	8.1	0.955	1.93	1.22	0.962	18.32	6.85	0.938
0.5α	26.54	6.70	0.975	2.24	1.09	0.957	24.29	5.61	0.960
0	29.84	8.20	0.930	0.59	1.51	0.946	27.68	6.86	0.965
0.1β	25.68	9.54	0.935	3.42	1.57	0.950	24.25	7.74	0.984
0.3β	37.93	6.98	0.940	5.19	1.07	0.982	31.90	5.99	0.966
0.5β	40.69	8.30	0.958	6.35	1.21	0.965	34.23	7.06	0.975

of w_e. However, the w_{ey} for both NAs-nucleated CPP and $\beta' w_{py}$ for α-NA nucleated CPP varied totally different from w_e, as w_{ey} for both nucleated CPP increased with increasing NAs while $\beta' w_{py}$ for α-NA nucleated CPP gradually decreased. Only the plastic component before yielding for β-NA nucleated CPP showed the same variation as βw_p did. Obviously, the component in the stage of necking and tearing was much higher than that in the stage of yielding, which indicated that the fracture properties were mainly determined by the necking and tearing process.

The crystallinity of these samples obtained form the DSC test are listed in Table II, and the dependence of the fracture parameters on crystallinity of the nucleated CPP are summarized in Figure 4. The crystallinity of nucleated CPP was calculated as follows:

$$X_c = \frac{\Delta H}{\Delta H_0} \tag{6}$$

where ΔH_0 was the heat of fusion for 100% crystalline CPP, ΔH was the measured heat of fusion for CPP in the nucleated CPP. The heat of fusion of 100% crystalline α- and β-CPP were 177.0 and 168.5 J/g, respectively.[37]

As shown in Table II and Figure 4, though the crystallinity for α-NA nucleated CPP was higher than that of β-NA nucleated CPP with the same content of 0.3 and 0.5 wt %, the variation of fracture toughness for both NAs-nucleated CPP versus crystallinity was similar. However, the down-trend of w_e for α-NA nucleated CPP at low crystallinity corresponding to low NA content (0.1 wt %) was more profound than that of β-NA nucleated CPP at low crystallinity resulting from low content of β-NA (0.1 wt %) incorporated, while the up-trend with increasing crystallinity as α-NA content increased was far less remarkable than that with increasing crystallinity as β-NA content increased. At the same time, the effect of crystallinity on the plastic work of both nucleated CPPs was also similar. As can be seen, the plastic work was the highest at the relative low crystallinity both for 0.1 wt % α- and β-NAs nucleated CPP. Then, the βw_p showed a down-trend with increasing crystallinity in both NAs-nucleated CPPs, although a fluctuation was presented for β-NA nucleated CPP at the content of 0.3 wt %.

As reported, β-NA can induce the transition of crystal from α-form to β-form, which is also reflected in Table III. The data in Table III were obtained according to eq. (7)[38] using the WAXD (shown in Fig. 5) results. K_β was the content of β-crystal in nucleated CPP, and I_β and I_α were the relative intensity corresponding to characteristic diffraction planes of CPP α- and β-crystal obtained from WAXD tests.

$$K_\beta = \frac{I_\beta(300)}{I_\beta(300) + I_\alpha(110) + I_\alpha(040) + I_\alpha(130)} \tag{7}$$

The crystallization of the NA-modified CPP mainly adopted a heterogeneous nucleation process, and the growth of β-crystals was governed by the number of nuclei existed in the system. The diagrams of fracture parameters as a function of K_β of β-NA nucleated CPP are presented in Figure 6. From the values listed in Table III, the variation of K_β exhibited an evident increasing trend which

TABLE II
The Crystallinity of CPP Modified by α- and β-NA at Different Content

Content (wt %)	Crystallinity (%)
0	34.7
0.1α	46.4
0.3α	48.8
0.5α	49.2
0.1β	47.3
0.3β	47.6
0.5β	48.0

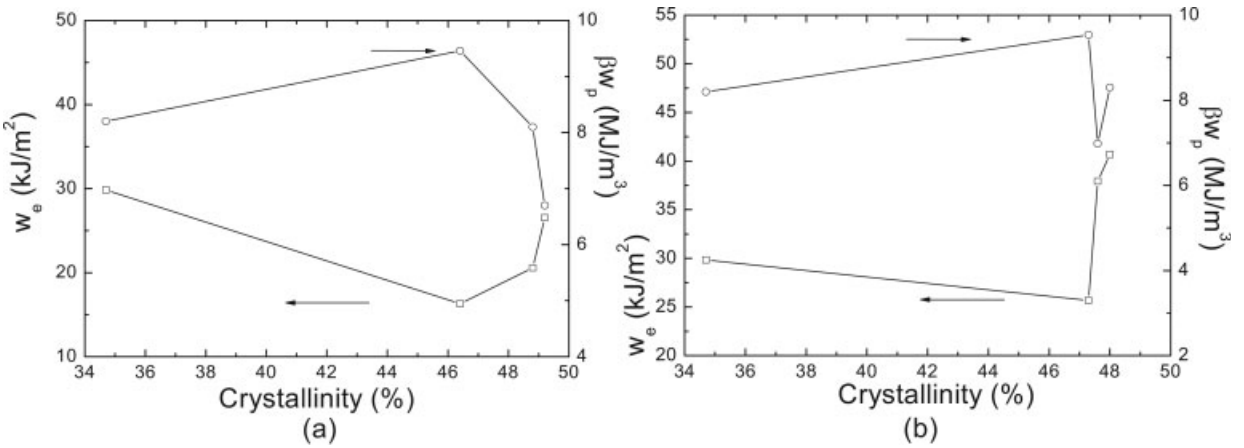

Figure 4 Fracture parameters against crystallinity for CPP modified by: (a) α and (b) β-NA at different content (□) w_e (○) βw_p.

could also be reflected from the diminishing I_α, indicating that elevating amount of NA led to the increasing β-content and consequently improved fracture resistance, which was consistent with β-crystal toughening mechanism. The reason why β-polypropylene crystals can improve the toughness of polypropylene can be attributed to a combined effect of several factors, including the α- to β-phase transformation induced by mechanical load, enhanced mechanical damping of polypropylene, and the peculiar lamellar morphology of polypropylene.[39]

When the content of NA reached 0.5% the diffraction peaks of α(040) and α(130) in the WAXD pattern was completely depressed, resulting in the prominence of β(300) peak and consequently elevation of K_β. For pure CPP, the w_e value was higher than those of β-NA nucleated CPP. With the addition of 0.1% NA, the w_e value of β-NA nucleated CPP decreased dramatically compared with that of pure CPP. However, as the NA content increases, the values of w_e increased gradually. This growing trend was coincident with the illustration of Figure 4(a). It was worth noting that the w_e value showed an obvious rise, when the NA content exceeds 0.3%, while this kind of dramatic variation appeared as the NA content was higher than 0.1%. The variation trend of βw_p values was also similar to Figure 4(a). For the CPP modified by 0.1% NA, its βw_p value reached the climax, whereas, the K_β value was not the highest. With the growing of K_β values, the βw_p value was declining.

CONCLUSIONS

Focusing on the effect of NA of different type and content on the fracture behavior of CPP, the following conclusions were drawn.

1. With the addition of NA, the crystallinity of both α- and β-modified CPP increased remarkably and the β-NA successfully induced the transition of CPP crystal from α-form to β-form.
2. The w_e values of CPP added with α-NA of different amount were all lower than that of pure CPP. The w_e values increased with further increase of α-NA amount. However, the βw_p was the highest at the lowest α-NA amount (0.1 wt %), while decreased with further increasing amount. The variation of w_{en} and $\beta'' w_{pn}$ with increasing NA content for α-NA nucleated PP was absolutely same as those of w_e and w_{ey} did, while the $\beta' w_{py}$ for α-NA nucleated PP gradually decreased. The plastic work decreased with increasing crystallinity in α-NA nucleated CPP.

Both w_e and βw_p showed similar trend of variation with increasing amount of β-NA. Only the plastic component before yielding for β-NA nucleated PP

TABLE III
Content of β-crystal in β-NA modified CPP

NA content (wt %)	$I_{\beta(300)}$ (%)	$I_{\alpha(110)}$ (%)	$I_{\alpha(040)}$ (%)	$I_{\alpha(130)}$ (%)	K_β (%)
0.1β	100.00	22.70	11.28	64.02	50.51
0.3β	100.00	12.55	0	44.37	63.73
0.5β	100.00	21.43	0	0	82.35

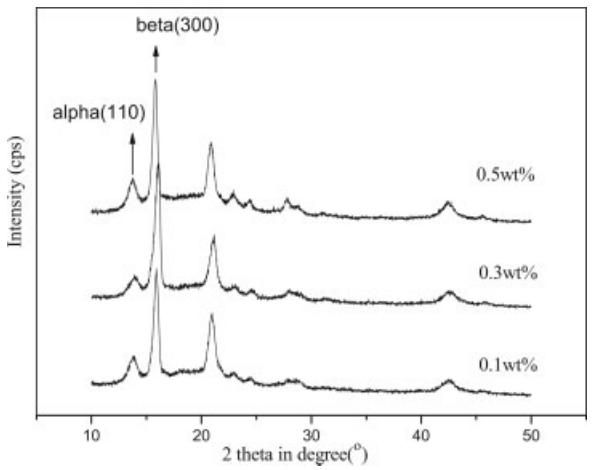

Figure 5 Effect of loading content of β-type NA on the WAXD patterns of CPP.

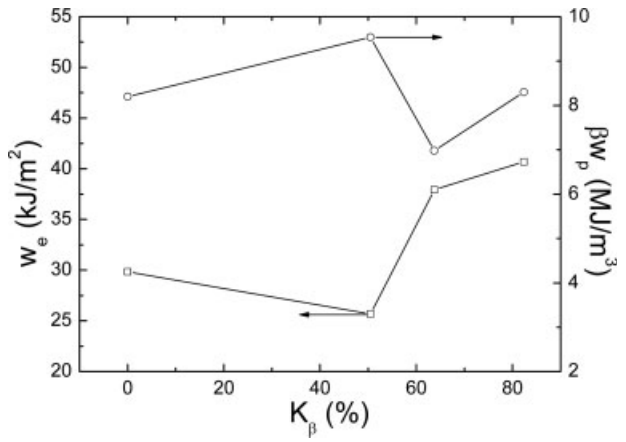

Figure 6 Specific work of fracture against K_β for CPP modified by β-NA at different content (□) w_e (○) βw_p.

had the same variation as βw_p. While the plastic work decreased first and then recovered close to that of pure CPP, with increasing crystallinity for β-NA nucleated CPP. The variation of K_β for NA-nucleated CPP was almost same as that of w_e, indicating that elevating amount of NA lead to the increase of β-content and consequently improved fracture resistance. The difference in the variation of βw_p value in CPP filled with β-NA may be due to the conversion of crystal form.

References

1. Wong, S. C.; Mai, Y. W. Polym Eng Sci 1999, 39, 356.
2. Mouzakis, D. E.; Gahleitner, M.; Karger-Kocsis, J. J Appl Polym Sci 1998, 70, 873.
3. Mouzakis, D. E.; Harmia, T.; Karger-Kocsis, J. Polym Polym Compos 2000, 8, 167.
4. Karger-Kocsis, J. J Macromol Sci Phys B 1999, 38, 635.
5. Gong, G.; Xie, B.-H.; Yang, W. Polym Test 2005, 24, 410.
6. Gong, G.; Xie, B.-H.; Yang, W. Polym Test 2006, 25, 98.
7. Xie, B.-H.; Shen, Y.-X.; Yang, W. Acta Polym Sci 2006, 2, 335.
8. Yang, W.; Xie, B.-H.; Yang, M.-B. J Mater Sci 2005, 40, 5323.
9. Yang, W.; Xie, B.-H.; Yang, M.-B. J Appl Polym Sci 2006, 99, 1781.
10. Nagarajan, K.; Levon, K.; Myerson, A. S. J Therm Anal Calorim 2000, 59, 497.
11. Karger-Kocsis, J.; Varga, J. J Appl Polym Sci 1996, 62, 291.
12. Hashemi, S. Polym Eng Sci 2000, 40, 798.
13. Tjong, S. C.; Xu, S. A.; Mai, Y. W. Mater Sci Eng 2003, 347, 338.
14. Mouzakis, D. E.; Gahleitner, M.; Karger-Kocsis, J. J Appl Polym Sci 1998, 70, 873.
15. Arkhireyeva, A.; Hashemi, S. Polymer 2002, 43, 289.
16. Mouzakis, D. E.; Karger-Kocsis, J. Polym Bull 1999, 42, 473.
17. Karger-Kocsis, J.; Ferrer-Balas, D. Polym Bull 2001, 46, 507.
18. Marchal, Y.; Oldenhove, B.; Daoust, D. Polym Eng Sci 1998, 38, 2063.
19. Karger-Kocsis, J.; Czigany, T. Polym Eng Sci 2000, 40, 1809.
20. Broberg, K. B. Int J Fract 1968, 4, 11.
21. Cotterell, B.; Reddel, J. K. Int J Fract 1977, 13, 267.
22. Mai, Y. W.; Cotterell, B. Int J Fract 1986, 32, 105.
23. Mai, Y. M.; Cotterell, B.; Horlyck, R.; Vigna, G. Polym Eng Sci 1987, 27, 804.
24. Mai, Y. W.; Powell, P. J Polym Sci Part B: Polym Phys 1991, 29, 785.
25. Wu, J.-S.; Mai, Y. W.; Cotterell, B. J Mater Sci 1993, 28, 373.
26. Wong, J. S. S.; Ferrer-Balas, D.; Li, R. K. Y.; Mai, Y. W.; Maspoch, M. L.; . Sue, H. J. Acta Mater 2003, 51, 4929.
27. Ferrer-Balas, D.; Mai, Y. W. Polymer 2001, 42, 2665.
28. Karger-Kocsis, J.; Barany, T.; Moskala, E. J. Polymer 2003, 44, 5691.
29. Karger-Kocsis, J.; Barany, T. Polym Eng Sci 2002, 42, 1410.
30. Karger-Kocsis, J.; Moskala, E. J. Polymer 2000, 41, 6301.
31. Karger-Kocsis, J.; Mouzakis, D. E. Polym Eng Sci 1999, 39, 1365.
32. Karger-Kocsis, J. Polym Bull 1996, 37, 119.
33. Karger-Kocsis, J.; Czigany, T.; Moskala, E. J. Polymer 1997, 38, 4587.
34. Karger-Kocsis, J.; Czigany, T.; Moskala, E. J. Polymer 1998, 39, 3939.
35. Karger-Kocsis, J.; Moskala, E. J. Polym Bull 1997, 39, 503.
36. Maspoch, M. L.; Gamez-Perez, J.; Karger-Kocsis, J. Polym Bull 2003, 50, 279.
37. Li, J. X.; Cheung, W. L.; Jia, D. M. Polymer 1999, 40, 1219.
38. Grein, C. Adv Polym Sci 2005, 188, 43.
39. Varga, J. J Macromol Sci Phys B 2002, 41, 1121.